The Energy Loss Straggling of low Z Ions in Solids and Gases

C. C. Montanari and J. E. Miraglia

Instituto de Astronomía y Física del Espacio, Consejo Nacional de Investigaciones Científicas y Técnicas and Universidad de Buenos Aires, Pabellón IAFE, Ciudad Universitaria, 1428 Buenos Aires, Argentina

Abstract. We present a study on the energy loss straggling of low Z ions (H up to B) in different solid (Al, Ti, Cu, Zn, Ge, Au) and gaseous targets (Ne, Ar, Kr, Xe). This work includes on one side, a critical analysis of the available experimental data and possible non-statistical (rugosity and inhomogeneity) contributions. On the other side, theoretical calculations performed by using the shell-wise local plasma approximation and the comparison of these results with the experimental data and with other theoretical curves available in the literature. We find that for the ions here considered, the square of the energy loss straggling normalized to Bohr limit is independent of the ion nuclear charge and of the ion charge state, in the case of electrons bound to the projectile. This shows a clear Z^2 dependence of the square energy loss straggling, with Z being the ion nuclear charge. The tendency to Bohr limit at high energies, and the inconvenience of using Yang formula (Q. Yang *etal*, *Nucl. Instrum. Meth. Phys. Res* B **61**, 149-155 (1991)) are also mentioned. The bases for the future development of a general formula for the energy loss straggling are introduced.

Keywords: Straggling, energy loss, dielectric formalism, inhomogeneity.

PACS: 34.50.Bw

INTRODUCTION

The dispersion in the energy loss, or energy loss straggling is an interesting parameter to study, both theoretically and experimentally. It is a sensitive input for many calculations [1] and simulation codes, like SIMNRA [2] for material analysis, or SEICS [3-4] for elements of biological interest.

There is an intrinsic energy loss straggling of statistical nature: when swift charged particles penetrate matter, they lose energy almost entirely through inelastic collisions with the electrons of the stopping material in a large number of collisional events, giving rise to the dispersion in the ion energy loss spectrum. However, the measured straggling includes also the contribution of surface roughness and inhomogeneity in the foil thickness [5-6]. It is present, for example, in some old data compiled by in Yang *et al* in 1991 [7]. One of the first studies on this non-statistical contribution to the energy loss straggling was performed by Besenbacher, Andersen and Bonderup in 1980 [8].

For the mean value of the energy loss, or stopping power, there are important compilations of data available in the web [9] and well-known and tested semi-empirical [10] and *ab-initio* quantum-mechanical codes [11]. Also different theoretical models [12-15] and recommended values [16] can be consulted. For the straggling in the energy loss the situation is quite different. The most extensively used expression is the analytical-empirical formulae by Yang [7], which is included in many ion beam analysis codes [17] (SIMNRA, NDF, CORTEO, MCERD, among others). The accuracy of this formula is questioned for different reasons [18-19], but the main one is that the source of Yang fitting is a compilation of data previous to 1980, which does not consider the influence of inhomogeneity.

Measurements of energy loss straggling set severe requirements to the target preparation, i.e. well defined thin films, uniformity and homogeneity [20]. Roughness and inhomogeneity of the samples introduce important additional energy loss straggling [6,8,20,21] in a region around the stopping maximum [8] and an important dispersion among data. The consequences of this contribution in the experimental values can be clearly noted in some measurements previous to 1980. In the last thirty years, a large number of straggling measurements have being obtained from different laboratories and techniques, which weight and subtract the non-statistical straggling from their data, showing less spread and tending to be close to a single band [22-28].

In this work we show the possibilities of the shell-wise local plasma approximation (SLPA) to deal with the straggling in the energy loss of ions in a media, which may be solid or gaseous. The SLPA is a many-electron model within the dielectric formalism, especially suitable for multi-electronic targets and high energy collisions [15,29]. This model describes the electronic response of each sub-shell of target electrons as a whole, including screening among electrons [30]. The main characteristics of the SLPA are the independent-shell approximation through a dielectric function for each sub-shell of target electrons and the explicit inclusion of the binding energy (not free-electron gas, but electron gas with an energy threshold). The SLPA is an *ab initio* calculation (no parameters included) whose only inputs are the atomic densities of the different sub-shells and the corresponding binding energies (Hartre-Fock wave functions and energies). It allows not only the calculation the energy loss straggling, but also ionization cross sections and stopping power.

THE SHELL-WISE LOCAL PLASMA APPROXIMATION

General Description and Ranges of Validity

The quantum dielectric formalism, a many-body consistent treatment for an ion in a homogeneous free-electron gas, has been developed by Lindhard [31] and by Ritchie [32]. This formalism, valid within the linear response approximation (LRA), was extended to deal with atomic bound electrons as a free-electron gas of local density in the local plasma approximation (LPA). It was applied to stopping power of heavy ions in matter using the logarithmic high energy limit [33-35]. Later developments of this model included the extension to isolated atoms by Rosseau, Chu and Powers [36], and to intermediate energies with the fully dielectric formulation [37-44]. Chu [45] employed the LPA for energy loss straggling calculations by using the full dielectric formalism and Hartree-Fock-Slater charge distribution for the target atom.

In the original LPA [33-45], the response of bound electrons is described as a whole by using the total density of electrons in the atom. This gives rather good description at high energies, but too low values at intermediate energies, as we will see in what follows.

The SLPA has two main differences with respect to the LPA: the first one is the independent shell approximation, by considering a separate dielectric response for each shell. Physically, this means that when an electron of the *nl* sub-shell is ionized only the other *nl*-electrons are included in the screening of the ion potential. A previous independent shell proposal is the orbital LPA (OLPA) by Meltzer *et al* [46] that uses the logarithmic high energy limit for the stopping power.

The second improvement is the inclusion of the ionization threshold with the Levine and Louie dielectric function [47]. This let us to use the SLPA not only for energy loss calculations, but for ionization cross section too, i.e. for inner-shell of metals, insulators [48] and gases [49]. The SLPA is an interesting alternative to the independent electron models, with great advantages in the computational effort and time, and very good results as compared with complex formulations such as the continuum distorted wave eikonal initial state (CDW-EIS) approximation [50].

The Levine-Louie dielectric function [47] keeps the virtues of Lindhard one [31]: electron-electron correlation to all orders, collective response, and *f*-sum rule (particle number conservation). The SLPA with Levine-Louie dielectric function has been employed with good results in stopping power calculations [15, 51-55] in an extended energy range, and in inner-shell ionization cross sections of very heavy targets at high impact velocities [29].

It must be noted that the SLPA is a perturbative description (first order approximation, with the dielectric functions calculated in LRA, like Lindhard's [31], Mermin's [56] or Levin-Louie's [47]), valid for $Z_P / v < Z_T$ and $v > v_e$, with v_e being the mean velocity of the electrons of each *nl* sub-shell.

The independent shell approximation is a proposal in the midway between the *full* free-electron-gas description of all target electrons, like the LPA, and the independent electron models in the binary formalism. As any approximation, even though reasonable, it is valid within certain limits. In this case the criteria to decide which electrons are considered together, including screening among them, and which not is the equal binding energy (within the energy uncertainty of the quantum mechanics). This was panned out in Refs. [15] and [54] when dealing with stopping in very heavy (relativistic) targets like W, Au, Pb or Bi. In these cases close binding energy, like those coming from the spin-orbit split, were considered together. The development of a dielectric function that includes the

screening among different shells depending on the impact velocity is pending.

The Energy Loss Straggling Calculation

The theoretical square energy loss straggling, Ω^2, describes the statistical dispersion of the energy loss. It represents the energy loss variance per unit path length of a Gaussian-type energy loss distribution [8], which is obtained when the energies transferred in the individual collisions are small as compared to the width of the final distribution [57].

The high energy limit for the energy loss straggling was developed by Bohr in 1915 [58]. For a bare ion of charge Z_P in collision with Z_T free electrons (i. e. at sufficiently high energies all target electrons are active in the collision) Bohr expression is

$$\Omega_B^2 = 4\pi Z_P^2 Z_T N\Delta x \qquad (1)$$

with N and Δx being the density of target atoms and the width, respectively.

Within the dielectric formalism, the square energy loss straggling per unit length is

$$\frac{\Omega^2}{N\Delta x} = \frac{2Z_P^2}{\pi v^2} \int_0^\infty \frac{dk}{k} \int_0^{kv} \omega^2 \, d\omega \;\; \mathbf{Im}\left[\frac{-1}{\varepsilon(k,\omega)}\right] \qquad (2)$$

The characteristics of the SLPA formulation are embodied in the calculation of the dielectric function through the following expression

$$\mathbf{Im}\left[\frac{-1}{\varepsilon(k,\omega)}\right] = \sum_{nl}\int d\vec{r} \;\; \mathbf{Im}\left[\frac{-1}{\varepsilon_{LL}(k,\omega,\delta_{nl}(r),E_{nl})}\right] \qquad (3)$$

where *nl* are the quantum numbers of the sub-shells, $\delta_{nl}(r)$ and E_{nl} are the density of the *nl*-electrons in the target atom and their binding energy. The dielectric function ε_{LL} is the Levine-Louie's [47], which includes explicitly the energy gap of each sub-shell. It is defined as

$$\mathbf{Im}\left[\varepsilon_{LL}(k,\omega,\delta_{nl},E_{nl})\right] = \begin{cases} \mathbf{Im}\left[\varepsilon_L(k,\omega_g,\delta_{nl})\right] & if\ \omega > |E_{nl}| \\ 0 & if\ \omega < |E_{nl}| \end{cases} \qquad (4)$$

with $\omega_g = \sqrt[2]{\omega^2 + E_{nl}^2}$ and with ε_L being the Lindhard dielectric function [31]. If we consider no binding energy ($E_{nl} = 0$) the usual expression for the probability in the dielectric formalism is recovered. The real part $\mathbf{Re}\left[\varepsilon_{LL}(k,\omega,\delta_{nl},E_{nl})\right]$ is obtained in closed form through the Kramers-Kronig relation, as shown in Ref. [47].

This dielectric function satisfies the so-called *f*-sum rule (particle number conservation) that is the desirable feature for a dielectric function.

The densities of electrons in the shells, $\delta_{nl}(r)$, and the binding energies, E_{nl}, are the only inputs for the SLPA. For atoms with nuclear charge Z<54, they can be obtained from the Hartree-Fock wave functions tabulated by Clementi and Roetti [59] or by Bunge *et al* [60]. For very heavy atoms (Z>54, such as Au in this contribution) they are calculated using the relativistic solutions of the Schrödinger equation [15, 29].

RESULTS AND DISCUSSION

Straggling in Solids

In Figures 1-6 we display our SLPA square straggling, calculated by using Eq. (2), and normalized to Bohr value, given by Eq. (1). In all the cases we compare with other theoretical calculations and also with the experimental values. The experimental data included has been carefully analyzed. In all the cases we include the measurements that explicitly correct the values by taking into account the contributions due to rugosity and inhomogeneity of the foil. This is an extra contribution that increases the experimental values giving overvalued measurements. Pioneering works on this subject were developed in the 80s by Besenbacher *et al* [8], Kido and coworkers [5, 23-24], and Eckardt and Lantschner [6, 27, 61].

All target electrons have been considered in the SLPA results displayed in Figs. 1-6, even very deep bound electrons (i.e. K-shell of Au). At sufficiently high energies each shell contributes to the total square energy loss straggling with a value proportional to the number of electrons in the shell, as predicted by Bohr [58]. If we express the square straggling as

$$\Omega^2 / \Omega_B^2 = \sum_{nl} \Omega_{nl}^2 / \Omega_B^2 \qquad (5)$$

adding each *nl* sub-shell contribution [15, 18], each term verifies that

$$\Omega_{nl}^2 / \Omega_B^2 \rightarrow N_{nl} / Z_T \qquad (6)$$

with N_{nl} being the number of electrons in the *nl* sub-shell. Eq. (6) gives the high energy limit expected for each shell, but it also represents a demanding requirement for the theoretical calculation, because even deep shells contribute to the total straggling, *i.e.* the 1s and 2s sub-shells of Cu are 10% of the energy loss straggling at 4 MeV, and tend to 14% at higher energies.

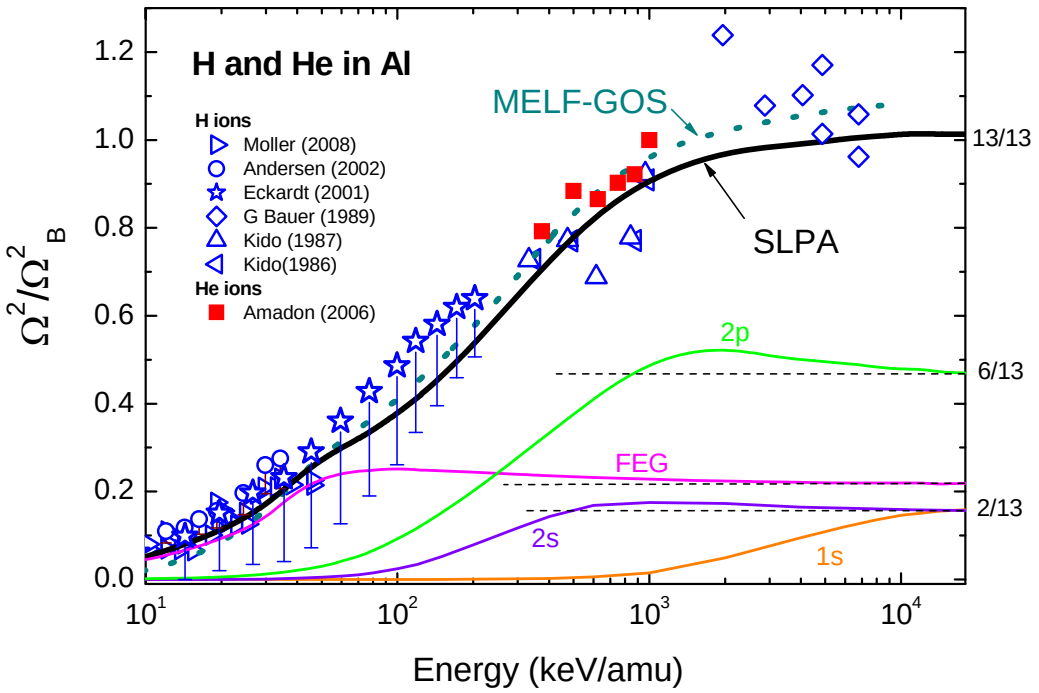

FIGURE 1. [color online] Squared energy loss straggling for H and He ions in Al, normalized to Bohr high energy limit. Curves: thick solid-line, present SLPA results; dotted-line, MELF-GOS calculations [18], thin solid lines, the SLPA for the different sub-shells. Symbols: experimental data as indicated in the figure. For H in Al [5,23,27,63-65]; for He in Al [26].

We present in Fig. 1 our results for H and He ions through Al foil, including the total square straggling normalized to Bohr, Ω^2 / Ω_B^2, and the shell contributions $\Omega_{nl}^2 / \Omega_B^2$, as indicated in Eqs. (5) and (6). The description of the experimental measurements is rather good. It can be noted that the data for He ions by Amadon *et al* [26] seems to follow the same curve as the proton data. We do not include in this figure the data compiled by Yang et al [7] for H and He in Al because it is experimental data previous to 1980, which does not consider corrections for inhomogenity or roughness of the sample. Similar comments may be done about the values for He in Al by Friedland and Lombard [62]. The values by Kido et al in 1983 [21] were measured again by the same group of authors taking into account the extra contributions [5, 23] and correcting the values. The differences among Kido previous and new results are clear in Fig. 4 of Ref. [18]. We also compare in Fig. 1 present SLPA curve with the MELF-GOS calculations by Abril and coworkers in Ref. [18], showing good agreement between the theoretical results. On the other hand, these values are rather different from those obtained with the largely employed formula by Yang et al [7]. This formula was obtained by fitting the old sets of experimental data not included in Fig. 1 because they include non-statistical contributions related with the samples employed. The inclusion of the different contributions in Fig. 1 show an interesting behavior: the straggling due to the interaction with the electrons of each sub-shell, Ω_{nl}^2, saturates to the value pedicted in Eq. (6), but shows a small overshooting before reaching it. This behavior is similar to that found in the case of low-Z targets (H and He) by Grande and Schiwietz [66] using a numerical solution of the Schrödinger equation. However, the total straggling of multielectronic targets seems to compensate the

overshooting of the different sub-shells, and the total straggling does not show this behavior. The experimental values displayed in Fig.1 support this statement. Moreover, the straggling measurements in different targets (Ti, Cu, Zn, Ge, Au, Ne, Ar, Kr, and Xe) that will be displayed along this work, strengthen this proposed.

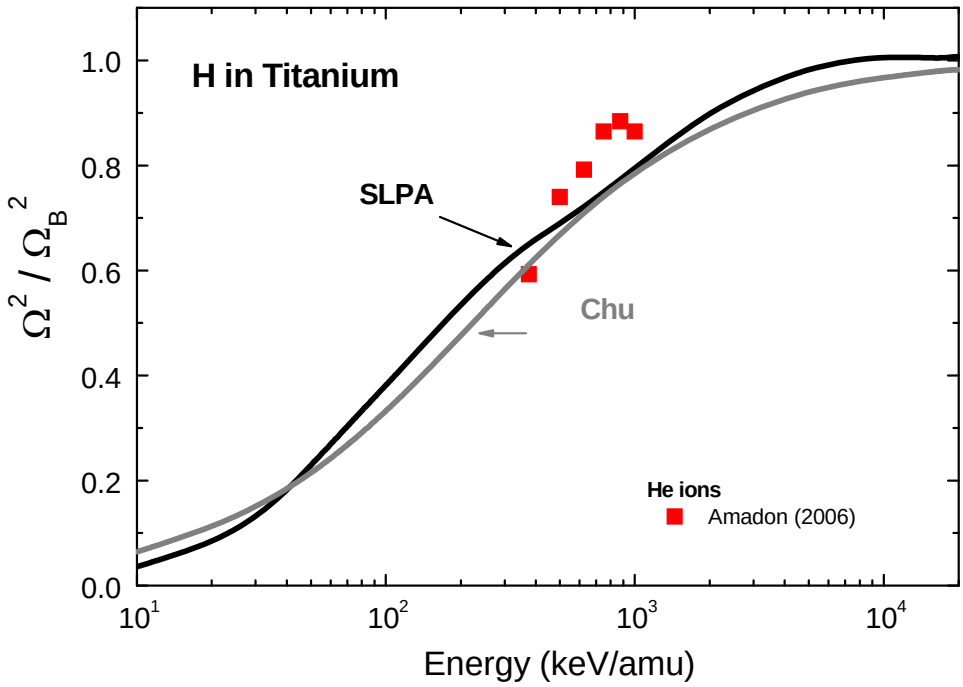

FIGURE 2. [color online] Squared energy loss straggling for H and He ions in Ti, normalized to Bohr high energy limit. Curves: black solid-line, present SLPA results; grey solid-line, Chu results [45]. Symbols: experimental data by Amadon *et al* [26].

Similar SLPA results are displayed in Fig. 2 for Ti target. In this case we only found experimental values for He ions in Ti by Amadon [26]. We include in this figure the comparison with the theoretical results by Chu [45] using the LPA with Hartree-Fock densities and considering the electronic cloud as a whole. The difference between our results and those by Chu [45] is the shell-to-shell description of the dielectric response, which gives SLPA values above Chu ones, except for low energies (E<40 keV).

In Fig. 3 we display the SLPA results in Cu including available data for H up to Li ions. The agreement between the SLPA results and the experimental data is good, the inclusion of H, He and also Li ions in this figure shows the week dependence of the normalized straggling with the ion charge, or the Z_P^2 dependence of the energy loss straggling. As in Fig. 1, we compare the SLPA values with the theoretical predictions of the MELF-GOS in Ref. [18] with very good agreement. We do not include in Fig. 3 the experimental data by Hoffman *et al* [67] in 1976 and by Friedland *et al* [68] in 1981, which are not corrected to exclude the inhomogeneity contribution. The overshooting of these values is clear, mainly in the data by Hoffman *et al* [67] as compared to recent measurements by Amadon [26].

Another case of interest is Zn, despite the few available experimental data. We display in Fig. 4 our results using the SLPA, together with alternative theoretical predictions by Chu [45] and by Arbo *et al* [70]. In the case of Arbo *et al* [70], the calculations were performed using the CDW-EIS for the solid inner-shells and the dielectric formalism for the valence electrons as a free electron gas. It can be observed in this figure that the experimental values by Eckardt in Ref. [70] tend to overestimate the straggling. The long down error bars account for the inhomogeneity contribution.

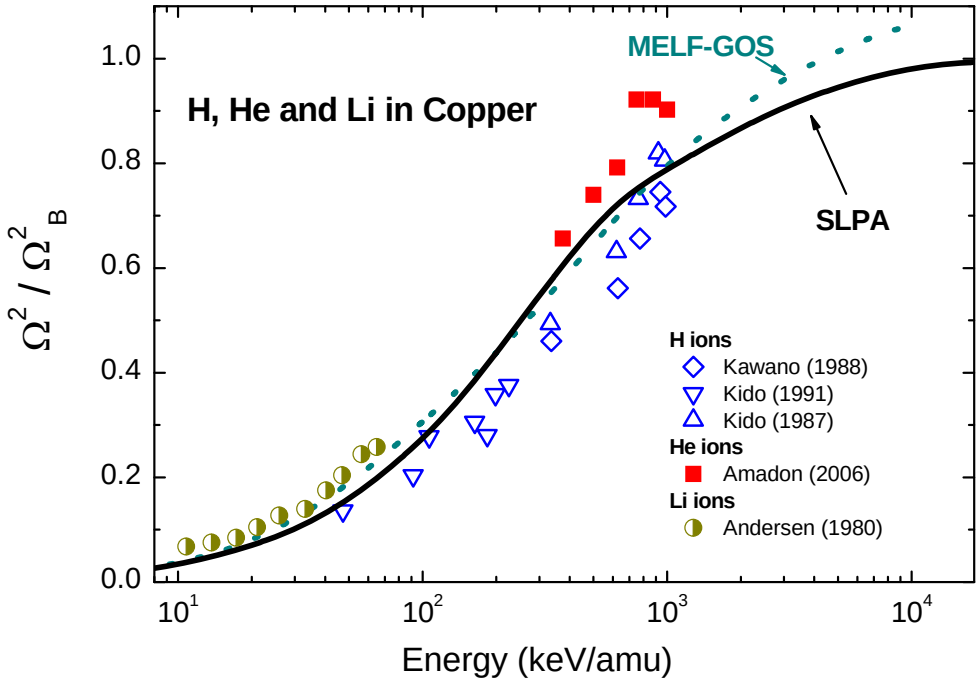

FIGURE 3. [color online] Squared straggling of Cu for H and He ions, normalized to Bohr high energy limit. Curves: solid-line, present SLPA results; dotted-line, MELF-GOS calculations [18] by Abril and coworkers. Symbols, experimental data as indicated in the figure: For H in Cu [23-25]; for He in Cu [26], and for Li in Cu [69].

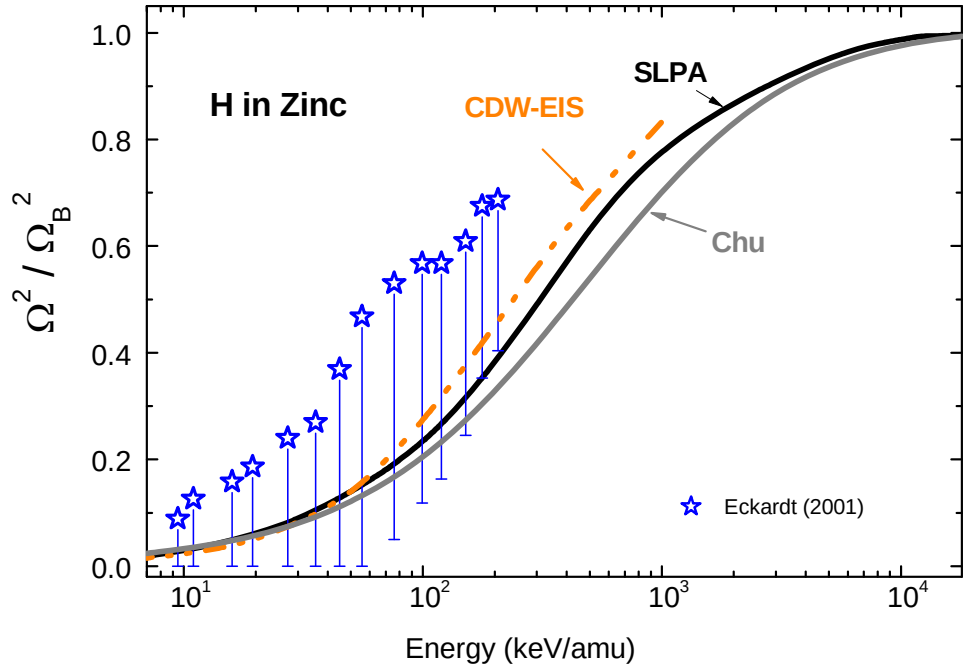

FIGURE 4. [color online] Squared energy loss straggling for H ions in Zn, normalized to Bohr high energy limit. Curves: black solid-line, present SLPA results; grey solid-line Chu values [45]; dashed-double dotted-line, CDW-EIS for the inner-shell contribution [70]. Symbols: experimental data by Eckardt and coworkers in Ref. [70].

In Fig. 5 we display the SLPA energy loss straggling of H and He ions in Ge. The comparison with the experimental data by Eckardt [61] and by Malherbe and Albert [71] is very interesting. In both cases, Eckardt [61] on one side and Malherbe and Albert [71] on the other, the straggling values for H and He ions normalized to Bohr agree quite well. The Ge sample by Malherbe and Albert [71] included rougosity, as mentioned by these authors. Comparisons with the theoretical results and with Eckardt [61] data also indicate some degree of overestimation in the measurements by Malherbe and Albert [71]. We include in the same figure two theoretical descriptions, the curve by Sigmund *et al* [72] using the binary theory for He ions, and the curve by Chu [45] using the LPA. As already noted, the SLPA values are close but above Chu ones [45]. On the other hand, the binary theory results seem to overestimate the data.

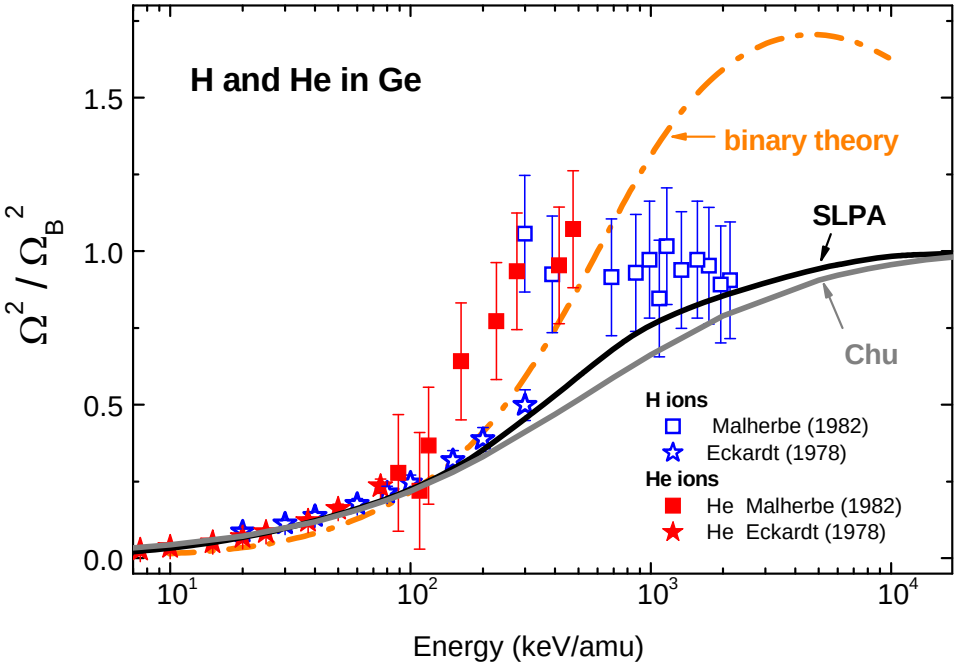

FIGURE 5. [color online] Square energy loss straggling, normalized to Bohr high energy limit. Curves: black solid-line, present SLPA results; grey solid-line Chu values [45]; dashed-dotted-line, binary theory by Sigmund *et al* [72] for He in Ge. Experimental data: for H and He ions by Eckardt [61] and Malherbe *et al* [71].

In Figure 6 we plotted together the experimental data for H up to B ions in Au together with the SLPA results. As for the other targets we only include the experimental data that explicitly take into account the roughness and inhomogeneity of the sample. In the case of the low energy measurements by Andersen *et al* [63], they have been corrected in 10 % due to the estimation of this contribution. We can observe that the week dependence of the experimental data normalized to Bohr with the ion charge is valid at least for H, He and Li ions. The data for B in Au by Hsu *et al* [22] could indicate a deviation for higher Z-ions. On the other hand, Figure 6 emphasizes the good description of the straggling obtained with the SLPA, even for unexpected low energies.

Present SLPA calculations correspond to bare ions. No considerations were done of different charge states of the ions inside the solid. This approximation is reasonable for low-Z ions because close collisions dominate the straggling (high ω probabilities are the main contribution in Eq. (2), while low ω values are canceled due to ω^2 dependence). This means that the interaction of target electrons with the ion nucleus is the main factor, giving similar results for the bare ion or for an ion with bound electrons. The experimental measurements for low-Z ions in multielectronic targets probe that this approximation holds almost in the whole energy range considered in this work. The limit of validity of this approximation for higher-Z ions may be one of the reasons for the separation of the data of B from the other ions in Fig. 6.

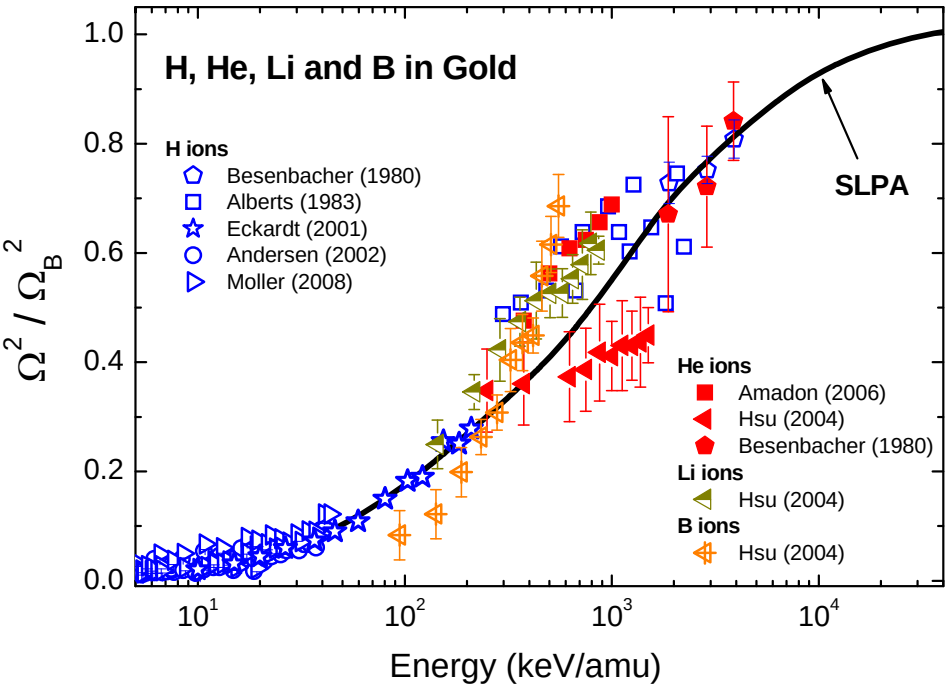

FIGURE 6. [color online] Squared straggling of Au for H, He, Li and B ions, normalized to Bohr high energy limit. Curves: solid-line, SLPA straggling for bare ions. Symbols: indicated in the figure; for H ions [8,27,28,63,64]; for He ion [8,22,26]; for Li and B ions [22].

While employing the SLPA for the different moments of the energy loss, we have found that even in the case of He ions, ionization cross sections and stopping cross sections are very different for He^0 or He^{2+} [51]. However, this is not the case for the energy loss straggling as observed in Figs. 1, 3 and 5. The inclusion of the screening of the projectile nucleus by its bound electrons within the SLPA can be found in Ref. [29] for inner-shell ionization. An analytical expression of the screened projectile charge $Z_P(Z_N,N_e,r)$ as a function of the distance to the nucleus r, the nuclear charge Z_N and number of bound electrons N_e, can be found in [29]. A tabulation of $Z_P(Z_N,N_e,r)$ for ions He up to Ne is included in [73].

We remark the differences between the results displayed in Figs 1-6 and those by Yang *et al* [7]. In fact present values are closer to Chu results [45] than to Yang *et al* [7]. The latter intends to correct Chu values by adding a term that fits experimental data, which in fact include extra-inhomogeneity contribution. The second term in Yang empirical formula adds certain overshooting to the straggling proportional to the stopping power [6, 8].

because the straggling measurements are cleaner and do not include the inhomogeneity contribution.

In Fig. 7 we display the SLPA straggling of protons in Ne, Ar, Kr and Xe, and compare them with experimental data by Besenbacher *et al* [8] and by Bonderup [35], and with the theoretical results by Chu [45]. Note that for gases the electronic energy loss is related not only to ionization but to excitation as well. We used the SLPA expressions given by Eqs. (2)-(4) with the energy gap equal to the first excited state (E_{3s}= -0.18 a.u. for Ne; E_{4s}= -0.17 a.u. for Ar; E_{5s}= -0.16 a.u. for Kr; E_{6s}= -0.15 a.u. for Xe).

Straggling in Gases

The development the SLPA is related to the energy loss in solid targets. However there is no reason to restrict its use *only* to solid targets. The response of bound electrons employed is based on the atomic wave functions and binding energies, described in full Hartree-Fock methods. On the other hand, calculations of energy loss straggling in gases have an extra interest

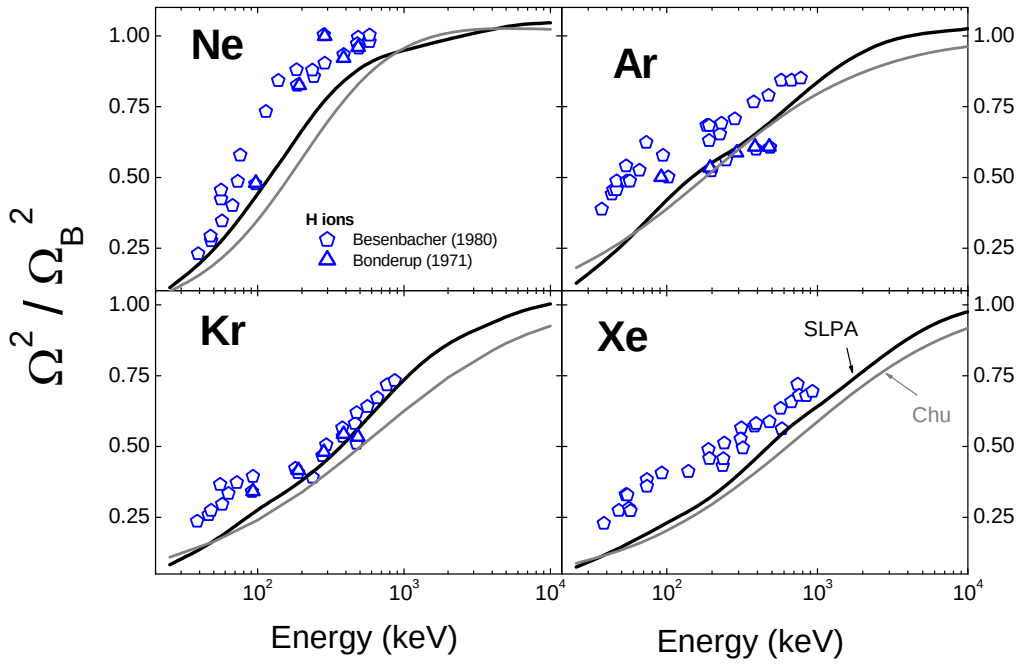

FIGURE 7. [color online] Normalized square energy loss straggling of protons in Ne, Ar, Kr and Xe. Curves: black solid line, present SLPA results, grey solid line, Chu straggling [45]. Symbols: experimental data by Besenbacher *et al* [8] and by Bonderup [35].

Our results are 15-20% below the experimental data by Besenbacher *et al* [8], except for Kr. The SLPA values are very sensitive to the energy gap considered, so this may indicate that the inclusion of the excitation channel needs further study. It can also be noted that in general the SLPA improves the LPA by Chu. This is a consequence of considering separate shells and the binding energies.

CONCLUSIONS AND FUTURE DEVELOPMENT

The energy loss straggling of ions in solid and gaseous targets has been analyzed using the theoretical description given by the SLPA. The experimental data available has been critically reviewed and only the straggling values that takes into account possible non-statistical contributions (rougosity and inhomogeneity of the samples) have been considered. This review of the experimental data shows the limitations of the largely used Yang formula for the straggling, which was obtained by fitting old experimental data non-corrected for inhomogeneity of the samples.

The SLPA results show good agreement with the experimental values, as far as the data agree among them. In the case of gaseous targets, where electron excitation must be included, the SLPA is around 15% below the measurements. In all the cases studied we obtained SLPA values that tend to the Bohr high energy limit.

The high energy prediction by Bohr shows that the square energy loss straggling tends to the number of active electrons, and this is valid for the total atom and for each shell too.

Finally, the energy loss straggling normalized to Z_P^2 (Bohr limit) is almost independent of the ion atomic number Z_P, at least for low-Z ions, showing a perturbative dependence with the ion charge.

Based on these results we will consider the future development of a simple analytical description for the energy loss straggling, based mainly in the review of the experimental data.

ACKNOWLEDGMENTS

This work was supported by the following Argentinian scientific organisms: CONICET (Consejo Nacional de Investigaciones Científicas y Técnicas), Universidad de Buenos Aires, and Agencia Nacional de Promoción Científica y Tecnológica.

REFERENCES

1. L. Ma, Y. Wang, J. Xue, Q. Chen, W. Zhang and Y. Zhang, J. App. Phys. 102 084702 (2007).
2. M. Mayer, SIMNRA Simulation program for the Analysis of NRA, RBS and ERDA, AIP Conference Proceedings 475, American Institute of Physics, Melville, NY, (1999), pp. 541, doi: 10.1063/1.59188; Nucl. Instrum. Methods. Phys. Res. B 194, 177 (2002)
3. S Heredia-Avalos and R Garcia-Molina, Phys. Rev. A 76 012901 (2007).
4. R. Garcia-Molina, I. Abril, S. Heredia-Avalos, I. Kyriakou and D. Emfietzoglou, Phys. Med. Biol. 56 6475 (2011).
5. Y Kido, Phys. Rev. B 34, 73 (1986).
6. J C Eckardt and G. H. Lantschner, Thin Solid Films 249, 11 (1994)
7. Q. Yang, D.J. O'Connor and Z. Wang, Nucl. Instr. Meth. Phys. Res. B 61, 149 (1991).
8. F Besenbacher , J. U. Andersen, and E. Bonderup, Nucl. Instrum. Methods 168, 1-15 (1980).
9. H. Paul, Stopping Power for Light Ions. Graphs, Data, Comments and programs in http://www.exphys.uni-linz.ac.at/stopping/
10. J. F. Ziegler, The stopping range of ions in matter, in http://www.srim.org
11. CasP version 5.0 (2011) available in http://www.helmholtz-berlin.de/people/gregor-schiwietz/casp_en.html; G. de Azevedo et al, Nucl. Instr. Meth. Phys. Res B 164, 203 (2000); and the improved UCA model in P.L. Grande and G. Schiwietz, Nucl. Instr. and Meth. Phys. Res. B 273, 1 (2012).
12. N. R. Arista and A. F. Lifschitz, in Advances in Quantum Chemistry, 45, 47 (J. Sabin ed., Elsevier, 2004).
13. P. Sigmund and A. Schinner, Nucl. Instr. Meth. Phys. Res B 195, 64 (2002).
14. S. Heredia-Avalos, J. C. Moreno-Marin, I. Abril, and R.Garcia-Molina, Nucl. Instr. Meth. Phys. Res B 230, 118 (2005).
15. C. C. Montanari, C.D. Archubi, D. M. Mitnik and J. E. Miraglia, Phys. Rev. A 79, 032903 (2009)
16. ICRU Report 49, International Commision on Radiation Units and Measurements (Bethesda, 1993)
17. N. P. Barradas, E. Rauhala, Data analysis software for Ion Beam Analysis, in Handbook of Modern Ion Beam Materials Analysis, edited by Y. Wang and M. Nastasi, MRS, Warrendale, Pennsylvania, 2009, pp. 307.
18. C. C. Montanari, J.E. Miraglia, S. Heredia-Avalos, R. Garcia-Molina, and I. Abril, Phys. Rev. A 75, 022903 (2007)
19. M. Msimanga, C.A. Pineda-Vargas, C.M. Comrie, S. Murray, Nucl. Instr. Meth. Phys. Res. B 273, 6 (2012).
20. D.W. Moon, H.I. Le, K.J. Kim, T. Nishimura and Y. Kido, Nucl. Instr. Meth. Phys. Res. B 183 10 (2001).
21. Y. Kido and T. Hioki, Phys. Rev. B 27, 2667 (1983).
22. J.Y. Hsu, Y.C. Yu, J.H. Liang, K.M. Chen and H. Niu, Nucl. Instrum. Meth. Phys. Res. B 219-220, 251 (2004).
23. Y. Kido, Nucl. Instr. Meth. Phys. Res. B 24-25, 347(1987).
24. Y. Kido and T. Koshikawa, Phys. Rev. A 44, 1759 (1991).
25. A. Kawano and Y. Kido, J. Appl. Phys. 63, 75 (1988).
26. S Amadon and W.A. Lanford, Nucl. Instr. Meth. Phys. Res. B 249 34 (2006).
27. J.C. Eckardt and G.H. Lantschner, Nucl. Instr. Meth. Phys. Res. B 175-177 93 (2001).
28. H.W. Alberts and J.B. Malherbe, Radiat. Effects 69 231 (1983)
29. C.C. Montanari, D. M. Mitnik and J. E. Miraglia, Rad. Eff. and Def. in Solids 166, 338 (2011).
30. P.M. Echenique, F. Flores, and R.H. Ritchie, Solid. State Phys. 43 229 (1990)
31. J. Lindhard, Mat. Fys. Medd. Dan. Vid. Selsk. 28, 1 (1954).
32. R.H. Ritchie, Phys. Rev. 114, 644 (1959).
33. J. Lindhard and M. Scharff, Mat. Fys. Medd. Dan. Vid. Selsk. 27 1 (1953).
34. J. Lindhard and A. Winther, K. Dan. Vidensk. Selsk. Mat. Fys. Medd. 34, 4 (1964).
35. E. Bonderup, Mat. Fys. Medd. Dan. Vid. Selsk. 35 1 (1967).
36. C.C. Rousseau, W.K. Chu, and D. Powers, Phys. Rev. A 4 1066 (1971).
37. C.M. Kwei, T.L. Lin, and C.J. Tung, J. Phys. B 21 2901 (1988).
38. C.J. Tung, R.L. Shyu, and C.M. Kwei, J. Phys. D 21, 1125 (1988).
39. Y.F. Chen, C.M. Kwei, and C.J. Tung, J. Phys. B 26, 1071 (1993).
40. J. Wang, R.J. Mathar, S.B. Trickey, and J.R. Sabin, J. Phys.: Condens. Matter 11, 3973 (1999).
41. W.K. Chu and D. Powers, Rev. Lett A 40, 23 (1972).
42. I. Gertner, M. Meron, and B. Rosner, Phys. Rev. A 21, 1191 (1980).
43. Y-N. Wang and T-C. Ma, Phys. Rev. A 50 (1994) 3192.
44. J.D. Fuhr, V.H. Ponce, F.J. García de Abajo and P.M. Echenique, Phys. Rev. B 57 (1998) 9329.
45. W. K. Chu, Phys. Rev A 13 2057-2060 (1976).
46. D.E. Meltzer, J.R. Sabin, and S.B. Trickey, Phys. Rev. A 41 (1990) 220.
47. Z.H. Levine and S.G. Louie, Phys. Rev. B 25 (1982) 6310.
48. A.J. Garcia and J.E. Miraglia, Phys. Rev. A 74, 012902 (2006).
49. C.D. Archubi, C.C. Montanari and J.E. Miraglia, J. Phys. B: At. Mol. Opt. Phys. 40, 943 (2007).
50. J.E. Miraglia and M.S. Gravielle, Phys. Rev. A 78 (2008) 052705.
51. Lantschner et al, Phys. Rev. A 69, 062903 (2004); C.C. Montanari et al, Phys. Rev. A 77, 042901 (2008).
52. E.D. Cantero, R.C. Fadanelli, C.C. Montanari, M. Behar, J. C. Eckardt, G.H. Lantschner, J.E. Miraglia and N.R. Arista, Phys. Rev. A 79, 042904 (2009).
53. C.C. Montanari and J.E. Miraglia, arXiv:0904.1386v1 [physics.atom-ph] (2009) Cornell University Library.
54. C.C. Montanari, D.M. Mitnik, C.D. Archubi, and J.E. Miraglia, Phys. Rev. A 80, 012901(2009).
55. E.D. Cantero, C.C. Montanari, M. Behar, R.C. Fadanelli, G.H. Lantschner, J.E. Miraglia and N.R. Arista, Phys. Rev. A 84 014902 (2011).
56. N.D. Mermin, Phys. Rev. B 1 (1970) 2362.

57. N. Bohr, K. Dan. Vidensk. Selsk. Mat. Fys, Medd. 24, 19 (1948).
58. N. Bohr, Phylos. Mag. 30, 581-612 (1915).
59. E. Clementti and C. Roetti, At. Data Nucl. Data Tables 14, 177 (1974).
60. C.F Bunge, J.A Barrientos, A.V Bunge and J.A Cogordan, Phys. Rev. A 46, 3691 (1992) 3691.
61. J.C. Eckardt, Phys. Rev. A 18, 426 (1978).
62. E. Friedland and J. M. Lombard, Nucl. Instrum. Methods 168, 25 (1980)
63. H.H. Andersen, A. Csete, T. Ichioka, H. Knudsen, S.P. Moller and U.I. Uggerhoj, Nucl. Instr. Meth. Phys. Res. B 194, 217 (2002).
64. S.P. Møller, A. Csete, T. Ichioka, H. Knudsen, H.-P.E. Kristiansen, U.I. Uggerhøj, H.H. Andersen, P. Sigmund and A. Schinner, Eur. Phys. J. D 46, 89 (2008) .
65. G.H. Bauer, A.J. Antolak, A.E. Pontau, D.H. Morse, D.W. Heikkinen, I.D. Proctor, Nucl. Instr. Meth. Phys. Res. B 43, 497-501 (1989).
66. P.L. Grande and G. Schiwietz, Phys. Rev. A 44, 2984 (1991).
67. G.E. Hoffman and D. Powers, Phys. Rev. A 13, 2042 (1976).
68. E. Friedland and C.P. Kotze, Nucl. Instr. Meth. Phys. Res. 191, 490 (1981).
69. H.H. Andersen, F. Besenbacher and P. Goddiksen, Nucl. Instr. Meth. Phys. Res. 168, 75 (1980).
70. D.G. Arbó, M.S. Gravielle, J.E. Miraglia, J.C. Eckardt, G.H. Lantschner, M. Famá and N. R. Arista, Phys. Rev. A 65, 042901 (2002).
71. J.B. Malherbe and H.W. Alberts, Nucl. Instrum. Meth. Phys. Res. B 192, 559-563 (1982).
72. P. Sigmund and A. Schinner, Europ. Phys. J. D 192, 201-209 (2002).
73. C.C. Montanari and J.E. Miraglia, The dielectric formalism for inelastic processes in high-energy ion-matter collisions, in *Advances in Quantum Chemistry*, Vol. 65, Chapter 7, edited by D. Belkic, Elsevier, in press (January 2013).